Triptycene-Based Polymers of Intrinsic Microporosity: Organic Materials That Can Be Tailored for Gas Adsorption

ARTICLE *in* MACROMOLECULES · MAY 2010

Impact Factor: 5.8 · DOI: 10.1021/ma100640m

Macromolecules
ARTICLE

Macromolecules **2010**, *43*, 5287–5294 **5287**
DOI: 10.1021/ma100640m

Triptycene-Based Polymers of Intrinsic Microporosity: Organic Materials That Can Be Tailored for Gas Adsorption

Bader S. Ghanem,[†,⊥] Mohammed Hashem,[†] Kenneth D. M. Harris,[†] Kadhum J. Msayib,[†] Mingcan Xu,[†] Peter M. Budd,[‡] Nhamo Chaukura,[‡] David Book,[§] Steven Tedds,[§] Allan Walton,[§] and Neil B. McKeown*[,†]

[†]*School of Chemistry, Cardiff University, Cardiff, CF10 3AT, U.K.,* [‡]*School of Chemistry, University of Manchester, Manchester, M13 9PL,U.K.,* [§]*School of Metallurgy and Materials, University of Birmingham, Birmingham, B15 2TT, U.K., and* [⊥]*Department of Chemistry, Taibah University, P.O. Box 344, Almadinah Almonawarah, Saudi Arabia*

Received March 23, 2010; Revised Manuscript Received May 1, 2010

ABSTRACT: We report the synthesis and properties of network polymers of intrinsic microporosity (network−PIMs) derived from triptycene monomers that possess alkyl groups attached to their bridgehead positions. Gas adsorption can be controlled by the length and branching of the alkyl chains so that the apparent BET surface area of the materials can be tuned within the range 618−1760 $m^2\ g^{-1}$. Shorter (e.g., methyl) or branched (e.g., isopropyl) alkyl chains provide the materials of greatest microporosity, whereas longer alkyl chains appear to block the microporosity created by the rigid organic framework. The enhanced microporosity, in comparison to other PIMs, originates from the macromolecular shape of the framework, as dictated by the triptycene units, which helps to reduce intermolecular contact between the extended planar struts of the rigid framework and thus reduces the efficiency of packing within the solid. The hydrogen adsorption capacities of the triptycene-based PIMs with either methyl or isopropyl substituents are among the highest for purely organic materials at low or moderate presures (1.83% by mass at 1 bar/77K; 3.4% by mass at 18 bar/77 K). The impressive hydrogen adsorption capacity of these materials is related to a high concentration of subnanometre micropores, as verified by Horvath−Kawazoe analysis of low-pressure nitrogen adsorption data.

Introduction

Microporous materials are solids that contain interconnected pores of less than 2 nm in size, and consequently, they possess large and accessible internal surface areas that can be exploited for heterogeneous catalysis, adsorption, separation and gas storage.[1] Conventional microporous materials consist of a crystalline inorganic framework (e.g., zeolites and related structures) or an amorphous structure (e.g., silica, activated carbon).[2,3] However, the impressive properties of crystalline organic−inorganic hybrid materials, such as the metal−organic-frameworks (MOFs),[4−11] has inspired the recent synthesis of purely organic porous materials such as the structurally related covalent−organic-frameworks (COFs)[12−17] and the study of microporous crystals derived from low molecular mass organic compounds.[18−22] Microporosity can also be obtained within amorphous organic materials, as demonstrated by hypercrosslinked polystyrenes,[23−27] and the recent extension of this concept to microporous polymer networks derived from a number of different monomers and polymerization reactions.[28−31] The open microporous structure of hypercrosslinked polymers arises from the formation of a solvent-swollen, rigid polymer network, which on removal of the included solvent does not collapse into a dense solid. Hypercrosslinked polymers can be made from a range of precursors, but those that exhibit the greatest microporosity (apparent BET surface area $>2000\ m^2\ g^{-1}$, pore volume $>1.5\ mL\ g^{-1}$) are those in which efficient network formation is achieved using Friedel−Crafts alkylation of chloromethylated polystyrene (e.g., Davankov resins),[32] or by polymerization of suitable aromatic monomers (e.g., *p*-xylylene-dichloride) using similar reaction conditions.[30]

In recent years, we have developed a class of microporous organic materials termed "polymers of intrinsic microporosity" (PIMs), based upon the concept of designing highly rigid and contorted macromolecules that cannot pack space efficiently in the solid state, thus leaving interconnected molecular-sized holes.[33−35] PIMs are not necessarily network polymers and a number of them (e.g., PIM-1; Scheme 1) are soluble in common solvents facilitating the fabrication of microporous films and coatings by solution processing.[36−40] These materials are promising for use in gas separation membranes as they demonstrate both high permeability and good selectivity for several gas pairs of commercial relevance (e.g., O_2/N_2 and CO_2/CH_4).[41,42] It was anticipated that combining the concept of hypercrosslinked network polymers with that of PIMs, by preparing network polymers using similar monomers and polymerization chemistry to those used for the preparation of soluble PIMs, would provide materials (i.e., network−PIMs) with greater microporosity. However, most of these network−PIMs demonstrate an apparent BET surface area significantly less than $1000\ m^2\ g^{-1}$.[43−48]

The rigid fused-ring framework and 3-fold symmetry of triptycene make it an attractive component for the synthesis of network PIMs with enhanced microporosity. Previously, triptycenes have been exploited widely as components of functional molecular systems including supramolecular receptors,[49−58] ligands,[59,60] molecular cages,[61] components for molecular machines (e.g., rotors, gyroscopes,[62−66] ratchets,[67−69] brakes[70,71] and gears[72,73]), technomimetic molecules[74,75] and materials such as liquid

*To whom correspondence should be addressed. E-mail: mckeownnb@cardiff.ac.uk. Telephone: +44 (0)2920-875851.

Published on Web 05/25/2010

Scheme 1. Synthesis of PIM-1[a]

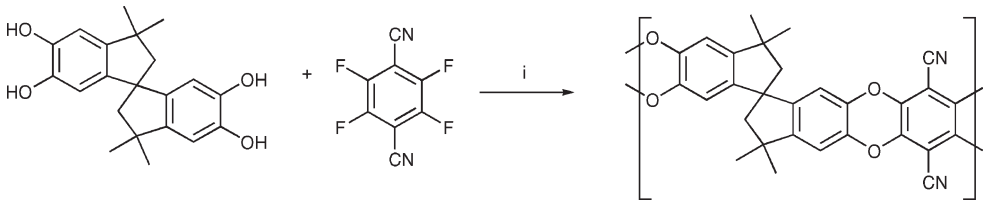

[a] Reagents and conditions: K_2CO_3, DMF, 60 °C, and 48 h.

Scheme 2. Synthesis of the Trip(R)−PIMs[a]

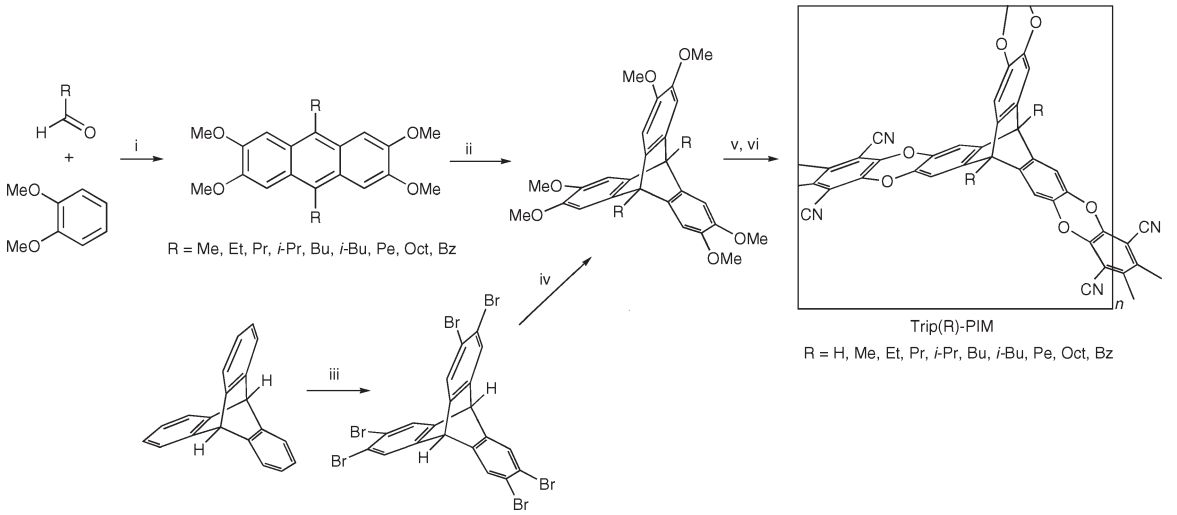

[a] Reagent and conditions: (i) cH_2SO_4, 5 °C, 2 h; (ii) diazonium salt of 4,5-dimethoxy-2-aminobenzoic acid, 1,2-epoxypropane, CH_2Cl_2, reflux, 12 h; (iii) Br_2, Fe CH_2Cl_2; (iv) MeONa, toluene, CuBr. v. BBr_3, CH_2Cl_2, room temperature, 3 h; (vi) 2,3,5,6-tetrafluoroterephthalonitrile, DMF, 80 °C, 24 h.

crystals,[76−78] clathrate crystals,[79−83] coordination networks,[84−87] and polymers.[88−92] Of particular interest to the development of novel microporous polymers is the concept of internal molecular free volume (IMFV), devised by Swager,[93] which suggests that the shape and width of the triptycene unit delineates a significant amount of unoccupied space.[94] This concept has been used to design useful functional materials by exploiting IMFV to obtain polymeric materials with large free volumes for applications as low-κ dielectric materials[95] and as a permeable matrix for nanoparticle fabrication.[96] Alternatively, liquid crystals or polymers can be obtained with enhanced alignment due to the minimization of IMFV via interlocking of the triptycenes.[78] It has also been demonstrated that the introduction of triptycene into a polymer can enhance its mechanical strength[97−99] and this too has been attributed to greater polymer cohesion due to the interlocking of the triptycene units. Structural building units with greater IMFV can be prepared by extending the triptycene system to give "iptycenes", a term introduced by Hart, to describe oligomeric systems that contain only fused arene and bicyclo[2,2,2]octane rings.[100−103] For example, the large amount of IMFV of the H-shaped pentiptycene can be used to design highly soluble, easily aligned, conjugated polymers with high free volumes that are beneficial for adsorbing aromatic molecules in fluorescence-based sensors.[98,104−110] It was noted by Hart that larger iptycenes (the term "polyiptycene" was coined)[101] would possess spacious cavities that may have applications as molecular hosts for adsorption.[102,111−113] In this context, recent work by Chong and MacLachlan has prepared oligomeric triptycenes some of which form amorphous states capable of significant nitrogen and hydrogen adsorption.[60,114]

Here we report the synthesis and properties of network−PIMs derived from triptycene monomers and we show that they possess enhanced microporosity, with surface areas that approach those of the best hypercrosslinked polymers but with a more defined structure containing a high concentration of micropores of subnanometre dimensions (i.e., ultramicropores).[115] In addition, the microporosity, and thus gas adsorption, of these materials can be controlled by the length and branching of the two alkyl chains attached to the polymer at the bridgehead positions of the triptycene subunits, thus allowing the apparent BET surface area of the polymers to be tuned over the range 600−1760 $m^2\ g^{-1}$. Hence these triptycene-based network−PIMs represents one of the few families of microporous material for which gas adsorption properties can be tailored exquisitely by subtle changes in structure.[116]

Experimental Section

Materials. Examples of synthetic procedures for the preparation of the triptycene monomers and their anthracene precursors are provided in the Supporting Information and are summarized in Scheme 2.

Example of the Synthesis of a Network-Triptycene PIM. Trip(Et)−PIM. To a stirred solution of 2,3,5,6-tetrafluoroterephthalonitrile (0.30 g, 1.5 mmol) and 9,10-diethyl-2,3,6,7,12,13-hexahydroxtriptycene (0.41 g, 1.0 mmol) in anhydrous DMF (70 mL) was added anhydrous potassium carbonate (9 mmol) as a fine powder. The mixture was then heated at 80 °C for 24 h under a nitrogen atmosphere. On cooling, the mixture was poured into water (300 mL) and acidified with 2 M HCl. The crude product was collected by filtration and washed with water and MeOH. Purification was achieved by stirring in refluxing MeOH and THF. The resulting orange solid was ground into a fine powder and dried in a vacuum oven at 100 °C for 16 h to give 0.63 g of Trip(Et)−PIMs (103% yield); IR (KBr cm^{-1}): ν = 3060, 3010, 2956, 2870 (C−H), 2235 (CN), 1610 (C−C Ar), 1170, 1250 (C−O); high-resolution solid state ^{13}C NMR (75.480 MHz): isotopic δ 8 (CH_3), 20 (CH_2), 53 (bridgehead *C*) 96 (*C*−CN), 112 (aromatic *C*−H), 135−155 (aromatic carbons).

Table 1. Gas Adsorption Data for the Trip(R)−PIMs

R	BET area ($m^2\ g^{-1}$)	N_2 uptake; (mmol g^{-1})	density (mL g^{-1})	H_2 uptake at 77 K, mmol g^{-1} (% mass)		
				1 bar	10 bar	calcd max.[a]
H	1318	22.8	1.57	7.46 (1.50)	11.8 (2.6)	19.9 (4.0)
Me	1760	42.2	1.67	8.90 (1.79)[b]	15.6 (3.2)	25.5 (5.2)
				6.30 (1.27)[c]	12.9 (2.6)[c]	
Et	1416[d]	39.5	1.40	8.33 (1.68)[b]	13.7 (2.8)	20.9 (4.2)
n-Pr	1343	32.1	1.40	7.69 (1.55)	12.2 (2.5)	17.6 (3.5)
i-Pr	1601	45.8	1.54	9.08 (1.83)	15.3 (3.1)	25.7 (5.2)
n-Bu	978	23.8	1.48	6.55 (1.32)	10.3 (2.1)	16.2 (3.2)
i-Bu	1076	24.5	1.43	7.34 (1.48)	11.7 (2.4)	17.5 (3.5)
Pe	947	17.9	1.48	5.61 (1.13)	8.8 (1.8)	13.8 (2.8)
Oct	618	11.6	1.27	3.67 (0.74)	6.0 (1.2)	9.3 (1.9)
benzyl	880	16.1	1.43	6.00 (1.20)	8.7 (1.7)	12.0 (2.4)

[a] Calculated H_2 saturation value using Sips equation.[136] [b] Volumetric measurement for H_2 uptake = 1.83% for Trip(Me)−PIM and 1.65% for Trip(Et)−PIM by mass at 1 bar (Micromeritics ASAP 2020). [c] Measurement at 87 K. [d] Mass measurement error resulted in this value being previously quoted as 1065 $m^2\ g^{-1}$.[115]

Anal. Found: C, 69.73; H, 3.02; N, 6.68; F, 0.88. Calcd for $C_{36}H_{16}N_3O_6$: C, 73.72; H, 2.75; N, 7.16; F, 0.00. (Note that after routine drying in a vacuum oven, TGA typically shows a loss of ~4−6% mass below 150 °C, probably due to adsorbed water or solvent. TGA analysis of samples for which rigorous removal of adsorbed species was achieved by prolonged exposed to high vacuum in the outgas port of the surface area analyzer at 120 °C gives a mass loss of < 0.5% mass below 100 °C).

High-Resolution Solid-State ^{13}C NMR Spectroscopy. Spectra were recorded at 293 K on a Chemagnetics CMX-Infinity 300 spectrometer (^{13}C frequency, 75.480 MHz) using a 4 mm triple-channel probe. The spectra were recorded under conditions of $^{13}C \leftarrow {}^{1}H$ cross-polarization, magic angle sample spinning and high power ^{1}H TPPM decoupling. In each experiment, 10000 scans were accumulated, with spinning frequency 6 kHz, CP contact time 5 μs and recycle delay 10 s. Dipolar dephasing ^{13}C NMR spectra[117] were recorded with dephasing delays of 40 and 60 μs.

Gas Adsorption Studies. Gas adsorption measurements were performed on samples that had been heated previously under ultra high vacuum (10^{-9} bar) at 100−120 °C for 8−12 h to remove residual solvent and other adsorbates. Basic volumetric N_2 sorption studies were undertaken at 77 K using a Beckman Coulter 3100 Surface Area Analyzer (Fullerton, California, USA). Low-pressure data, suitable for modeling micropore size distribution, were obtained using a Micromeritics Instrument Corporation (Norcross, GA) accelerated surface area and porosimetry (ASAP) 2020 system. Helium was used for the free space determination, after nitrogen sorption analysis, both at ambient temperature and at 77 K. Apparent surface areas were calculated from N_2 adsorption data by multipoint BET analysis. Apparent micropore distributions were calculated from N_2 adsorption data by the Horvath−Kawazoe method,[118] assuming a slit-pore geometry and the original H−K carbon-graphite interaction potential. Gravimetric H_2 sorption studies were undertaken using a Hiden Isochema (Warrington, Cheshire, U.K.) intelligent gravimetric analyzer (Hiden IGA-001), which incorporates an electronic microbalance capable of measuring mass change with a resolution of ±0.2 μg. After degassing, pressure composition isotherms were measured in ultrapure H_2 (Air Products 99.99995%, additionally passed through a liquid nitrogen trap) up to 18 bar at liquid nitrogen and liquid argon temperatures (77 and 87 K). The measured masses were corrected for buoyancy using the weights and densities of all the components on both sides of the balance. The sample density was measured using helium pycnometry using a Micromeritics AccuPyc II 1340 System (Table 1) with ultrapure helium (Air Products −99.99996%).

Results

Synthesis. The triptycene-based PIMs, denoted Trip(R)−PIMs (where R = bridgehead substituent), were prepared from the reaction between a 2,3,6,7,12,13-hexahydroxytriptycene monomer and commercially available 2,3,5,6-tetrafluoroterephthalonitrile (Scheme 2). With one exception (i.e., R = H), the triptycene monomers are readily prepared from the Diels−Alder reaction between 9,10-dialkyl-2,3,6,7-tetramethoxyanthracene and 4,5-dimethoxybenzyne (prepared *in situ* from the diazonium salt of 4,5-dimethoxy-2-aminobenzoic acid),[119] followed by demethylation of the 9,10-dialkyl-2,3,6,7,12,13-hexamethoxytriptycene product using BBr_3.[50,54] A range of 9,10-dialkyl-2,3,6,7-tetramethoxyanthracenes (R = Me, Et, Pr, *i*-Pr, Bu, *i*-Bu, *t*-Bu, Pe, Oct, Bz) was readily accessible from the simple reaction between the appropriate aldehyde and veratrole in cH_2SO_4, by slight modifications to published procedures.[120−122] Surprisingly, the triptycene-forming Diels−Alder reaction proved relatively unaffected by the presence of a branched alkyl chain or benzyl group at the 9,10-positions of the anthracene, thus allowing the synthesis of monomers with isopropyl or isobutyl groups attached to the bridgehead positions, although bulkier *tert*-butyl groups did prohibit the benzyne cycloaddition. In contrast, attempts to prepare the novel precursor 2,3,6,7,12,13-hexamethoxytriptycene (i.e., R = H) were unsuccessful due to the failure of the Diels−Alder reaction. Instead, it was prepared by the copper(I) bromide mediated reaction of 2,3,6,7,12,13-hexabromotriptycene[94] with sodium methoxide (Scheme 2).[123]

Each of the Trip(R)−PIMs was obtained as an insoluble yellow-orange powder in quantitative yield and was initially characterized by elemental analysis, from which the lack of residual fluorine ($F < 1.0\%$) indicates an efficient network formation. It should be noted that the network-forming reaction (i.e., a double aromatic nucleophilic substitution reaction) is the same as that used to prepare high molecular mass PIM-1 ($M_w > 1 \times 10^5$ g mol^{-1}) suitable for robust film formation (Scheme 1). High resolution solid state ^{13}C NMR (Figure 1) and IR spectra support the ideal structure of the networks depicted in Scheme 2. Powder X-ray diffraction confirms that the material is amorphous, as expected. thermal gravimetric analysis (TGA) of the Trip(R)−PIMs shows no decomposition below 400 °C.

Gas Adsorption. The N_2 adsorption isotherms for the Trip(R)−PIMs obtained at 77 K (e.g., Figure 2) show significant adsorption for each member of the series at low relative pressures ($p/p^o < 0.1$), consistent with microporosity. Apparent BET surface areas (Table 1), calculated from the isotherms, range from 618 $m^2\ g^{-1}$ (R = octyl) to 1760 $m^2\ g^{-1}$ (R = methyl). The total nitrogen uptake at $p/p^o = 1.0$ also displays a smooth trend across the homologous series, decreasing from 42.2 mmol g^{-1} to 11.6 mmol g^{-1} (Table 1 and Figure 3). Of interest is the effect of branched alkyl chains on the microporosity, with a greater BET surface area

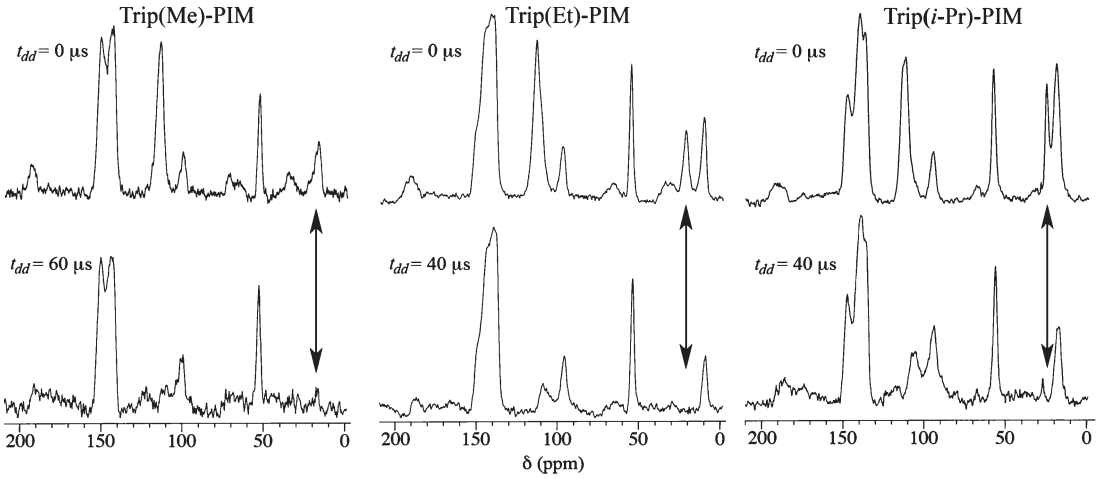

Figure 1. High-resolution solid-state ^{13}C NMR spectra for Trip(Me)−PIM, Trip(Et)−PIM and Trip(*i*-Pr)−PIM with upper spectra being standard ^{13}C NMR spectra (with no dipolar dephasing) and lower spectra obtained with dephasing delays (t_{dd} as indicated). The arrows indicate the signals due to the methyl, methylene and methine carbons, respectively, attached directly to the bridgehead positions of the triptycene. Complete suppression of these signals occurs in Trip(Et)−PIM and Trip(*i*-Pr)−PIM but not in Trip(Me)−PIM, as discussed in the text.

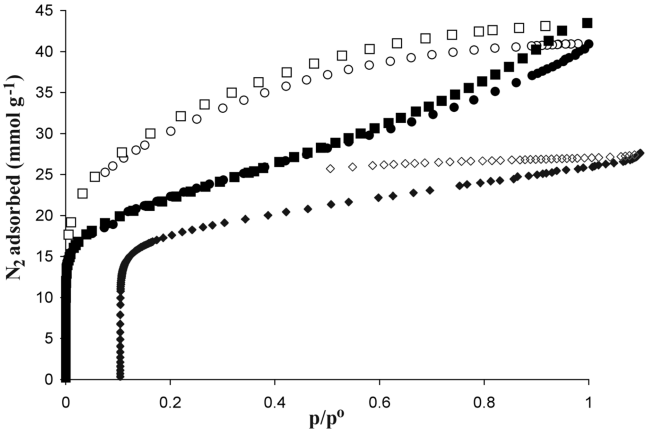

Figure 2. Nitrogen adsorption (solid symbols) and desorption (open symbols) isotherms for Trip(Me)−PIM at 77 K, obtained in Manchester (●) and Liverpool (■, data courtesy of Prof. Andrew I. Cooper and Dr. Colin Wood) and for Trip(H)−PIM (♦), with the values of the *X*-axis displaced by $p/p^o = 0.1$ for clarity. Good agreement was achieved between different laboratories; slight variations at high relative pressure may be attributed to textural differences between samples. Note the very pronounced hysteresis between the adsorption and desorption isotherms for Trip(Me)−PIM and the relatively small hysteresis for Trip(H)−PIM.

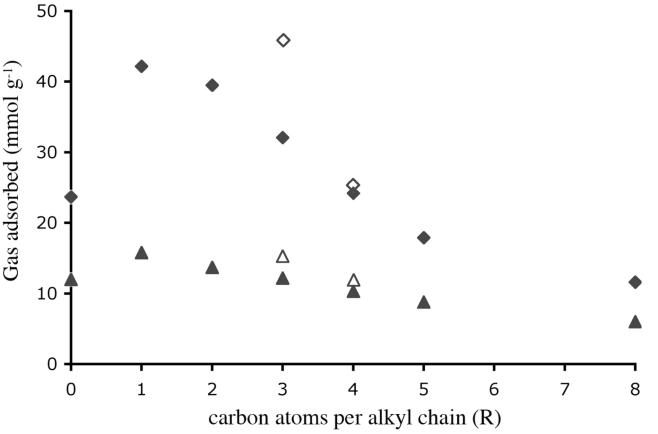

Figure 3. Amount of gas adsorbed within the Trip(R)−PIMs at 77 K versus the length of the alkyl chain (R; note that 0 corresponds to R = H) attached to the bridgehead position of the triptycene subunits (♦ N_2 at $p/p_o = 1.0$; ▲ H_2 at 10 bar). The filled symbols are for *n*-alkyl side-chains whereas empty symbols represent the data for Trip(R)−PIMs containing isopropyl and isobutyl.

and overall nitrogen uptake for Trip(*i*-Pr)−PIMs in comparison with Trip(*n*-Pr)−PIM. A smaller enhancement of microporosity is obtained for Trip(*i*-Bu)−PIM over Trip(*n*-Bu)-Trip. A particularly distinct feature of the adsorption isotherms, especially those of the Trip(R)−PIMs with shorter alkyl chains, is the pronounced hysteresis that extends to low relative pressures between the adsorption and desorption cycles (Figure 2). It is notable that the absence of a bridgehead alkyl substituent in Trip(H)−PIM reduces significantly the degree of hysteresis and the amount of N_2 adsorbed at $p/p^o = 1.0$, although this material is still highly microporous (apparent BET surface area = 1318 m^2 g^{-1}).

The values for H_2 adsorption are provided in Table 1 and Figure 3. A typical H_2 adsorption isotherm for Trip(*i*-Pr)−PIM is given in Figure 4. The isotherms are completely reversible and Type 1 in shape, as is typical for the physisorption of H_2 on microporous materials. Significant hydrogen adsorption was observed for each material, with Trip(Me)−PIM and Trip(*i*-Pr)−PIM displaying uptake in excess of 3% by mass at 10 bar.

Discussion

Gas adsorption demonstrates that the Trip(R)−PIMs possess a greater degree of microporosity relative to any PIM prepared previously (Table 1), with the exception of those possessing long (R = Pe, Oct) or bulky side-chains (R = Bz). Consideration of a molecular model of a fragment of Trip(Et)−PIM (Figure 5) reveals a possible explanation for this enhanced microporosity. The triptycene component constrains the growth of the polymer within the same plane, with the faces of the ribbon-like "struts" between the triptycenes being oriented perpendicular to the plane of the macromolecular growth. This arrangement may help to block face-to-face association between these planar struts and may thus help to frustrate further the space-efficient packing of the polymer network, leading to greater microporosity. The reduction in gas adsorption of Trip(R)−PIMs as the length of the *n*-alkyl groups is increased suggests that the flexible side-chains occupy an increasingly larger proportion of the free volume created by the rigid polymer framework. A similar pore-blocking effect has been reported recently for mesoporous alkyl-substituted COFs.[13] In contrast, the isopropyl side-chains do not diminish the microporosity. It is known that the architecture of triptycene imposes severe steric restrictions on the

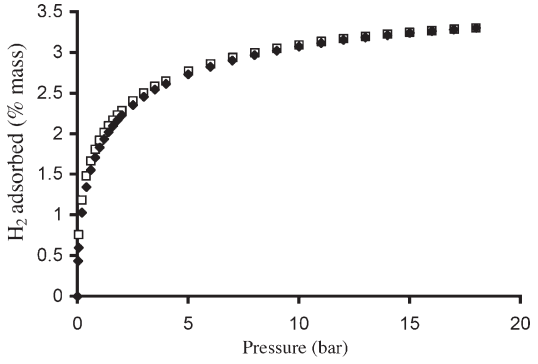

Figure 4. Hydrogen adsorption isotherm for Trip(*i*-Pr)−PIM obtained at 77 K (empty squares represents the desorption isotherm). Note the lack of hysteresis between the adsorption and desorption isotherms.

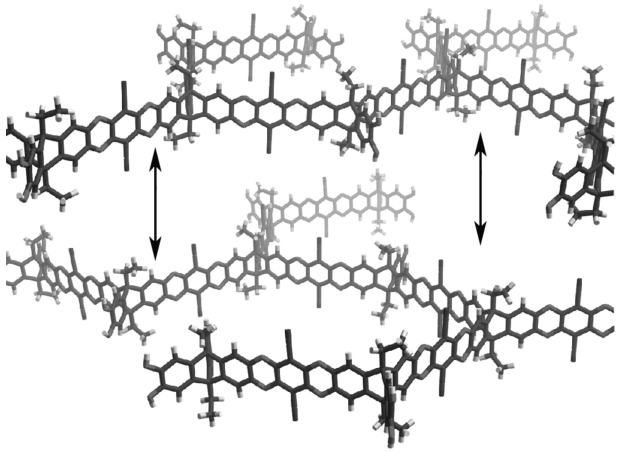

Figure 5. Representation of two ideal fragments of the network of Trip(Et)−PIM showing how the shape of each macromolecule, as dictated by the architecture of the triptycene units, prevents close intermolecular interactions between the planar "struts". The loose network which arises from the ideal layered structure may account for the tendency of the materials to swell in organic solvents or during nitrogen adsorption, as indicated by the arrows, especially when bridgehead alkyl chains block interpenetration of the nitrile groups.

motion of a short alkyl chain attached to the bridgehead carbon. The dipolar dephasing solid state ^{13}C NMR experiments, at 293 K, provide some direct qualitative insights regarding such reorientational dynamics of these alkyl groups within the Trip(R)−PIMs. For rigid organic solids, a dipolar dephasing delay of 40 μs is generally sufficient to suppress the ^{13}C NMR signal for a ^{13}C nucleus directly bonded to ^{1}H, but when a $^{13}C-^{1}H$ bond undergoes reorientational dynamics (as often observed in the case of methyl groups), a dipolar dephasing delay significantly longer than 40 μs is typically required to suppress the ^{13}C NMR signal. As can be see from Figure 1, the methyl groups in Trip(Et)−PIM and Trip(*i*-Pr)−PIM undergo significant reorientational dynamics, whereas the $^{13}C-^{1}H$ bonds in the methylene group of Trip(Et)−PIM and in the methine group of Trip(*i*-Pr)−PIM do not undergo significant reorientation.[124] For Trip(Me)−PIM, our results suggest that the methyl group undergoes reorientation, but that the reorientation is significantly more hindered than is typical for methyl groups in organic solids. Solution state NMR studies on triptycenes substituted with an isopropyl group at the bridgehead show that the activation energy for rotation about the $C-CH(CH_3)_2$ bond is in excess of 75 kJ mol^{-1}.[125−128] Hence, it can be concluded that ethyl and isopropyl side-chains are unable to alter their conformation in order to occupy free volume and can be considered as part of the rigid framework of the PIM, whereas longer *n*-alkyl side-chains have sufficient conformational freedom to fill the free volume.

The pronounced hysteresis between the adsorption and desorption isotherms of the Trip(R)−PIMs (Figure 2) extends to low relative pressure and is distinct from that associated with mesoporosity, which closes at a high relative pressure ($p/p^o > 0.4$).[129] For the Trip(R)−PIMs, the hysteresis may be caused by activated adsorption arising either from a continuous swelling of the material as nitrogen is adsorbed or from the restricted access of nitrogen molecules at lower relative pressures due to constricted pore openings or, most likely, a combination of both of these mechanisms. Swelling may be a particular feature of these networks because their *ideal* structure comprises two-dimensional meshes (including many macrocyclic structures) with no covalent attachment between the resulting macromolecular layers (Figure 5). In reality, defects and mechanical interlocking might provide a relatively small number of robust linkages between the layers, so that the material is likely to behave as a lightly cross-linked network. The swelling of the network may be facilitated by the relaxation of internal stress initially induced from the removal of solvent from the original solvent-swollen state as N_2 fills the micropores. It is notable that the hysteresis of the N_2 isotherm of Trip(H)−PIM is relatively small (Figure 2), which may be due to the strong dipolar interactions between interdigitated nitrile groups in different layers reducing swelling. In contrast, the bridgehead alkyl groups in the Trip(R)−PIMs are likely to block nitrile interdigitation and allow greater swelling of the network during N_2 adsorption.

The amount of hydrogen that can be loaded within the Trip(R)−PIMs containing shorter alkyl chains at moderate pressure (up to 3.4% by mass at 18 bar for Trip(Me)−PIMs) is significantly greater than that obtained for any PIM to date, and is comparable with the loadings obtained for other types of microporous materials with similar BET surface areas (Table 2) such as activated carbons (e.g., PICACTIF-SC),[130] hypercrosslinked polymers (e.g., CDX/BCMBP),[30] COFs (e.g., COF-5),[14] and MOFs (e.g., MOF-505).[131,132] However, activated carbons, MOFs, COFs and the recently reported porous aromatic framework (PAF-1)[133] with higher surface areas adsorb greater amounts of hydrogen (Table 2). It is notable that the loadings of hydrogen at low pressure (1 bar) within Trip(*i*-Pr)−PIM and Trip(Me)−PIMs are among the highest reported for purely organic polymers[134] and that these values are competitive with the best performing examples of other classes of porous materials. The impressive low pressure H_2 adsorption of the Trip(R)−PIMs can be attributed to a high concentration of pores with subnanometre dimensions, which are suitable for multiwall adsorption (Figure 5). Analysis of the low-pressure N_2 adsorption data of Trip(Me)−PIM, based on the Horvath−Kawazoe method,[118] confirms that the pore size distribution is strongly biased toward pores that are less than a nanometre in diameter (Figure 6). It has been noted previously that pores of diameter in the range 0.6 - 0.8 nm are optimal for hydrogen physisorption at low pressures for a range of microporous materials[132,135] including polymers.[29,46] The heat of adsorption for Trip(Me)−PIM, calculated using a Virial equation and isotherms at 77 and 87 K, is 6.5 kJ mol^{-1} at zero coverage and 5.2 kJ mol^{-1} at 8 mmol g^{-1} loading. Using the Virial analysis other microporous materials have given similar values (e.g., 6.2 and 7.0 kJ mol^{-1} for COF-1 and COF-6 respectively at zero surface coverage − both of which have a pore size of 0.9 nm).[12] Applying the Clausius−Clapeyron equation to the H_2 adsorption data for Trip(Me)−PIM obtained at 77 and 87 K gives a slightly higher range for the heat of adsorption of 8.8−6.0 kJ mol^{-1} for loadings of 0.1−1% mass H_2. This is a similar result (7.5−6.2 kJ mol^{-1}) to that obtained for the BCMBP/p-DCX hypercrosslinked polymer (median pore width = 0.89 nm) using the Clausius−Clapeyron equation.[30]

Table 2. Comparison of Hydrogen Loadings of Microporous Materials at 77 K

		H_2 uptake at 77 K (% mass)			
	BET area, $m^2\ g^{-1}$	1 bar	10 bar	maximum	ref
		PIMs			
Trip(Me)−PIM	1760	1.80	3.2	3.4 (18 bar)	
Trip(*i*-Pr)−PIM	1601	1.83	3.1	3.3 (18 bar)	
Porph−PIM	960	1.20	1.9	2.0 (18 bar)	46
CTC−PIM	770	1.35	1.7	1.7 (10 bar)	137
PIM-1	750	0.95	1.5	1.5 (18 bar)	137
OFP-3	1159	1.56 [1.40][a]	3.9 [2.2][a]	3.9 (10 bar)	138
poly(spirobisfluorene)	1043		2.3	3.7 (60 bar)	31
		Hypercrosslinked Polymers			
polystyrene	1930	1.40	3.1	5.2 (80 bar)	139, 140
polystyrene	1466	1.27	2.8	3.1 (15 bar)	141
DCX/BCMBP	1904	1.50	3.3	3.7 (15 bar)	30
BCMBP	1366	1.70	2.4	2.8 (15 bar)	134
polyaniline	630	0.80	1.7	2.2 (30 bar)	28
		COFs/PAFs			
COF-5	1590	0.9	2.4	3.6 (50 bar)	12, 14
COF-102	3620	1.20	5.8	7.2 (30 bar)	12
PAF-1	7100	∼1.5	∼4.5	7.0 (48 bar)	133
		Activated Carbons			
PICACTIF-SC	1700	1.90	3.0		130
AX-21	2421	2.40	4.0		130
zeolite-templated	3200	2.60	6.9		142
		MOFs			
Cu_2(bptc)/(MOF-505)	1670	2.59	3.7	4.0 (20 bar)	132, 143
Cu_2(qptc)	2932	2.24	5.3	7.0 (20 bar)	132
MIL-101	5500	2.50		6.1 (40 bar)	144
MOF-177	5640	1.25		7.5 (70 bar)	131

[a] Figure in brackets represent hydrogen loadings obtained for OFP-3 using the same instrument (Hiden, IGA-1) and conditions as those used for the Trip(R)−PIMs in this study. The unbracketed values were obtained previously using a Micromeritics ASAP 2050 surface area analyzer.[138] We thank Prof. Saad Makhseed, Kuwait University, for kindly supplying a sample of OFP-3.

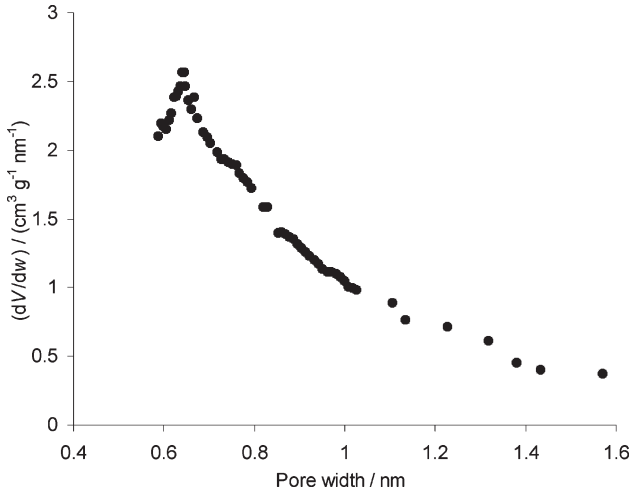

Figure 6. Micropore size distribution for Trip(Me)−PIM based on the Horvath−Kawazoe analysis of low-pressure nitrogen adsorption data (combined data from Figure 1) showing that the major contribution to porosity is from pores that are less than a nanometre in diameter.

For each Trip(R)−PIM, the amount of H_2 adsorbed at 10 bar is very similar to the amount of N_2 adsorption at low relative pressure ($p/p^o = 0.01$), as both values depend upon the number of accessible micropores. However, the total amount of N_2 adsorbed by the Trip(R)−PIMs with shorter or branched alkyl substituents is much greater due to the uptake in the higher relative pressure range $p/p^o = 0.1 - 1.0$ (Table 1, Figure 2). For example, for Trip(*i*-Pr)−PIM the amount of N_2 adsorbed at 1 bar (at 77 K) is three times the amount of H_2 adsorbed at 10 bar. The additional N_2 adsorption at higher relative pressure is associated with large hysteresis, which, as discussed above, is probably related to the swelling of the polymer network. Unfortunately, hydrogen adsorption does not give rise to a similar effect under the conditions used in this study, although it is possible that higher pressures or lower temperatures might enhance loadings via this mechanism. Studies to explore this possibility are in progress.

Acknowledgment. We are grateful to the EPSRC for funding (EP/D074312/1) and we thank Prof. Andrew I. Cooper and Dr. Colin Wood, University of Liverpool, U.K., for independent verification of the N_2 and H_2 adsorption isotherms for Trip(Me)−PIM.

Supporting Information Available: Text giving additional synthetic procedures and figures giving additional gas adsorption isoterms. This material is available free of charge via the Internet at http://pubs.acs.org.

References and Notes

(1) *Handbook of Porous Solids*; Schüth, F., Sing, K., Weitkamp, J., Eds.; Wiley-VCH: Berlin, 2002; Vol. *1*−*5*.
(2) Xu, R.; Pang, W.; Yu, J.; Huo, Q.; Chen, J. *The Chemistry of Zeolites and Related Porous Solids: Synthesis and Structure*; Wiley: Singapore, 2007.
(3) Wright, P. A. *Microporous Framework Solids*; RSC: Cambridge, U.K., 2007.

(4) Ockwig, N. W.; Delgado-Friedrichs, O.; O'Keeffe, M.; Yaghi, O. M. *Acc. Chem. Res.* **2005**, *38*, 176–182.
(5) Eddaoudi, M.; Kim, J.; Rosi, N.; Vodak, D.; Wachter, J.; O'Keefe, M.; Yaghi, O. M. *Science* **2002**, *295*, 469–472.
(6) Eddaoudi, M.; Moler, D. B.; Li, H.; Chen, B.; Reinke, T. M.; O'Keefe, M.; Yaghi, O. M. *Acc. Chem. Res.* **2001**, *34*, 316–330.
(7) Eddaoudi, M.; Li, H. L.; Yaghi, O. M. *J. Am. Chem. Soc.* **2000**, *122*, 1391–1397.
(8) Ferey, G. *Chem. Soc. Rev.* **2008**, *37*, 191–214.
(9) Ferey, G.; Mellot-Draznieks, C.; Serre, C.; Millange, F. *Acc. Chem. Res.* **2005**, *38*, 217–225.
(10) Ferey, G.; Mellot-Draznieks, C.; Serre, C.; Millange, F.; Dutour, J.; Surble, S.; Margiolaki, I. *Science* **2005**, *309*, 2040–2042.
(11) Kitagawa, S.; Kitaura, R.; Noro, S. *Angew. Chem., Int. Ed.* **2004**, *43*, 2334–2375.
(12) Furukawa, H.; Yaghi, O. M. *J. Am. Chem. Soc.* **2009**, *131*, 8875–8883.
(13) Tilford, R. W.; Mugavero, S. J.; Pellechia, P. J.; Lavigne, J. *J. Adv. Mater.* **2008**, *20*, 2741–2746.
(14) Han, S. S.; Furukawa, H.; Yaghi, O. M.; Goddard, W. A. *J. Am. Chem. Soc.* **2008**, *130*, 11580-+.
(15) El-Kaderi, H. M.; Hunt, J. R.; Mendoza-Cortes, J. L.; Cote, A. P.; Taylor, R. E.; O'Keeffe, M.; Yaghi, O. M. *Science* **2007**, *316*, 268–272.
(16) Cote, A. P.; El-Kaderi, H. M.; Furukawa, H.; Hunt, J. R.; Yaghi, O. M. *J. Am. Chem. Soc.* **2007**, *129*, 12914–129146.
(17) Cote, A. P.; Benin, A. I.; Ockwig, N. W.; O'Keeffe, M.; Matzger, A. J.; Yaghi, O. M. *Science* **2005**, *310*, 1166–1170.
(18) Comotti, A.; Bracco, S.; Distefano, G.; Sozzani, P. *Chem. Commun.* **2009**, 284–286.
(19) Thallapally, P. K.; McGrail, B. P.; Atwood, J. L.; Gaeta, C.; Tedesco, C.; Neri, P. *Chem. Mater.* **2007**, *19*, 3355–3357.
(20) Couderc, G.; Hertzsch, T.; Behrnd, N. R.; Kramer, K.; Hulliger, J. *Microporous Mesoporous Mater.* **2006**, *88*, 170–175.
(21) Sozzani, P.; Bracco, S.; Comotti, A.; Ferretti, L.; Simonutti, R. *Angew. Chem., Int. Ed.* **2005**, *44*, 1816–1820.
(22) Msayib, K. J.; Book, D.; Budd, P. M.; Chaukura, N.; Harris, K. D. M.; Helliwell, M.; Tedds, S.; Walton, A.; Warren, J. E.; Xu, M. C.; McKeown, N. B. *Angew. Chem., Int. Ed.* **2009**, *48*, 3273–3277.
(23) Pastukhov, A. V.; Tsyurupa, M. P.; Davankov, V. A. *J. Polym. Sci., Part B: Polym. Phys.* **1999**, *37*, 2324–2333.
(24) Tsyurupa, M. P.; Davankov, V. A. *React. Func. Polym.* **2006**, *66*, 768–779.
(25) Tsyurupa, M. P.; Davankov, V. A. *React. Func. Polym.* **2002**, *53*, 193–203.
(26) Davankov, V. A.; Tsyurupa, M. P. *React. Polym.* **1990**, *13*, 27–42.
(27) Davankov, V. A.; Tsyurupa, M. P. *Pure Appl. Chem.* **1989**, *61*, 1881–1888.
(28) Germain, J.; Frechet, J. M. J.; Svec, F. *J. Mater. Chem.* **2007**, *17*, 4989–4997.
(29) Germain, J.; Svec, F.; Frechet, J. M. J. *Chem. Mater.* **2008**, *20*, 7069–7076.
(30) Wood, C. D.; Tan, B.; Trewin, A.; Niu, H. J.; Bradshaw, D.; Rosseinsky, M. J.; Khimyak, Y. Z.; Campbell, N. L.; Kirk, R.; Stockel, E.; Cooper, A. I. *Chem. Mater.* **2007**, *19*, 2034–2048.
(31) Yuan, S. W.; Kirklin, S.; Dorney, B.; Liu, D. J.; Yu, L. P. *Macromolecules* **2009**, *42*, 1554–1559.
(32) Ahn, J. H.; Jang, J. E.; Oh, C. G.; Ihm, S. K.; Cortez, J.; Sherrington, D. C. *Macromolecules* **2006**, *39*, 627–632.
(33) McKeown, N. B.; Budd, P. M.; *Macromolecules* **2010**, DOI: 10.1021/ma1006396.
(34) McKeown, N. B.; Budd, P. M. *Chem. Soc. Rev.* **2006**, *35*, 675–683.
(35) McKeown, N. B.; Budd, P. M.; Msayib, K. J.; Ghanem, B. S.; Kingston, H. J.; Tattershall, C. E.; Makhseed, S.; Reynolds, K. J.; Fritsch, D. *Chem.—Eur. J.* **2005**, *11*, 2610–2620.
(36) Budd, P. M.; Elabas, E. S.; Ghanem, B. S.; Makhseed, S.; McKeown, N. B.; Msayib, K. J.; Tattershall, C. E.; Wang, D. *Adv. Mater.* **2004**, *16*, 456–460.
(37) Budd, P. M.; Ghanem, B. S.; Makhseed, S.; McKeown, N. B.; Msayib, K. J.; Tattershall, C. E. *Chem. Commun.* **2004**, 230–231.
(38) Carta, M.; Msayib, K. J.; Budd, P. M.; McKeown, N. B. *Org. Lett.* **2008**, *10*, 2641–2643.
(39) Ghanem, B. S.; McKeown, N. B.; Budd, P. M.; Fritsch, D. *Macromolecules* **2008**, *41*, 1640–1646.
(40) Ghanem, B. S.; McKeown, N. B.; Budd, P. M.; Selbie, J. D.; Fritsch, D. *Adv. Mater.* **2008**, *20*, 2766–2769.
(41) Budd, P. M.; McKeown, N. B.; Ghanem, B. S.; Msayib, K. J.; Fritsch, D.; Starannikova, L.; Belova, N.; Sanfirovad, O.; Yampolskii, Y.; Shantarovich, V. *J. Membr. Sci.* **2008**, *325*, 851.
(42) Budd, P. M.; Msayib, K. J.; Tattershall, C. E.; Ghanem, B. S.; Reynolds, K. J.; McKeown, N. B.; Fritsch, D. *J. Membr. Sci.* **2005**, *251*, 263–269.
(43) Budd, P. M.; Ghanem, B.; Msayib, K.; McKeown, N. B.; Tattershall, C. *J. Mater. Chem.* **2003**, *13*, 2721–2726.
(44) Mackintosh, H. J.; Budd, P. M.; McKeown, N. B. *J. Mater. Chem.* **2008**, *18*, 573–578.
(45) Maffei, A. V.; Budd, P. M.; McKeown, N. B. *Langmuir* **2006**, *22*, 4225–4229.
(46) McKeown, N. B.; Budd, P. M.; Book, D. *Macromol. Rapid Commun.* **2007**, *28*, 995–1002.
(47) McKeown, N. B.; Hanif, S.; Msayib, K.; Tattershall, C. E.; Budd, P. M. *Chem. Commun.* **2002**, 2782–2783.
(48) McKeown, N. B.; Makhseed, S.; Budd, P. M. *Chem. Commun.* **2002**, 2780–2781.
(49) Webster, O. W. *Macromol. Symp.* **1994**, *77*, 177–182.
(50) Zhu, X. Z.; Chen, C. F. *J. Am. Chem. Soc.* **2005**, *127*, 13158–13159.
(51) Han, T.; Chen, C. F. *Org. Lett.* **2006**, *8*, 1069–1072.
(52) Zong, Q. S.; Zhang, C.; Chen, C. F. *Org. Lett.* **2006**, *8*, 1859–1862.
(53) Zong, Q. S.; Chen, C. F. *Org. Lett.* **2006**, *8*, 211–214.
(54) Zhu, X. Z.; Chen, C. F. *Chem.—Eur. J.* **2006**, *12*, 5603–5609.
(55) Han, T.; Zong, Q. S.; Chen, C. F. *J. Org. Chem.* **2007**, *72*, 3108–3111.
(56) Han, T.; Chen, C. F. *J. Org. Chem.* **2007**, *72*, 7287–7293.
(57) Peng, X. X.; Lu, H. Y.; Han, T.; Chen, C. F. *Org. Lett.* **2007**, *9*, 895–898.
(58) Xue, M.; Chen, C. F. *Chem. Commun.* **2008**, 6128–6130.
(59) Azerraf, C.; Grossman, O.; Gelman, D. *J. Organomet. Chem.* **2007**, *692*, 761–767.
(60) Chong, J. H.; MacLachlan, M. J. *J. Org. Chem.* **2007**, *72*, 8683–8690.
(61) Zhang, C.; Chen, C. F. *J. Org. Chem.* **2007**, *72*, 9339–9341.
(62) Hou, S. M.; Sagara, T.; Xu, D. C.; Kelly, T. R.; Ganz, E. *Nanotechnology* **2003**, *14*, 566–570.
(63) Godinez, C. E.; Zepeda, G.; Garcia-Garibay, M. A. *J. Am. Chem. Soc.* **2002**, *124*, 4701–4707.
(64) Godinez, C. E.; Zepeda, G.; Mortko, C. J.; Dang, H.; Garcia-Garibay, M. A. *J. Org. Chem.* **2004**, *69*, 1652–1662.
(65) Caskey, D. C.; Wang, B.; Zheng, X. L.; Michl, J. *Collect. Czech. Chem. Commun.* **2005**, *70*, 1970–1985.
(66) Kelly, T. R.; Cai, X. L.; Damkaci, F.; Panicker, S. B.; Tu, B.; Bushell, S. M.; Cornella, I.; Piggott, M. J.; Salives, R.; Cavero, M.; Zhao, Y. J.; Jasmin, S. *J. Am. Chem. Soc.* **2007**, *129*, 376–386.
(67) Kelly, T. R.; Tellitu, I.; Sestelo, J. P. *Angew. Chem., Int. Ed.* **1997**, *36*, 1866–1868.
(68) Kelly, T. R.; Sestelo, J. P.; Tellitu, I. *J. Org. Chem.* **1998**, *63*, 3655–3665.
(69) Davis, A. P. *Angew. Chem., Int. Ed.* **1998**, *37*, 909–910.
(70) Kelly, T. R.; Bowyer, M. C.; Bhaskar, K. V.; Bebbington, D.; Garcia, A.; Lang, F. R.; Kim, M. H.; Jette, M. P. *J. Am. Chem. Soc.* **1994**, *116*, 3657–3658.
(71) Harrington, L. E.; Cahill, L. S.; McGlinchey, M. J. *Organometallics* **2004**, *23*, 2884–2891.
(72) Yamamoto, G. *Chem. Lett.* **1990**, 1373–1376.
(73) Nikitin, K.; Mueller-Bunz, H.; Ortin, Y.; Risse, W.; McGlinchey, M. J. *Eur. J. Org. Chem.* **2008**, 3079–3084.
(74) Jimenez-Bueno, G.; Rapenne, G. *Tetrahedron Lett.* **2003**, *44*, 6261–6263.
(75) Rapenne, G.; Jimenez-Bueno, G. *Tetrahedron* **2007**, *63*, 7018–7026.
(76) Norvez, S. *J. Org. Chem.* **1993**, *58*, 2414–2418.
(77) Norvez, S.; Simon, J. *Liq. Cryst.* **1993**, *14*, 1389–1395.
(78) Long, T. M.; Swager, T. M. *J. Mater. Chem.* **2002**, *12*, 3407–3412.
(79) Yang, J. S.; Liu, C. P.; Lee, G. H. *Tetrahedron Lett.* **2000**, *41*, 7911–7915.
(80) Lu, J.; Zhang, J. J.; Shen, X. F.; Ho, D. M.; Pascal, R. A. *J. Am. Chem. Soc.* **2002**, *124*, 8035–8041.
(81) Yang, J. S.; Liu, C. P.; Lin, B. C.; Tu, C. W.; Lee, G. H. *J. Org. Chem.* **2002**, *67*, 7343–7354.
(82) Soldatov, D. V. *J. Chem. Crystallogr.* **2006**, *36*, 747–768.
(83) Konarev, D. V.; Drichko, N. V.; Lyubovskaya, R. N.; Shul'ga, Y. M.; Litvinov, A. L.; Semkin, V. N.; Dubitsky, Y. A.; Zaopo, A. *J. Mol. Struct.* **2000**, *526*, 25–29.
(84) Munakata, M.; Wu, L. P.; Sugimoto, K.; Kuroda-Sowa, T.; Maekawa, M.; Suenaga, Y.; Maeno, N.; Fujita, M. *Inorg. Chem.* **1999**, *38*, 5674–5680.
(85) Wen, M.; Munakata, M.; Suenaga, Y.; Kuroda-Sowa, T.; Maekawa, M. *Inorg. Chim. Acta* **2002**, *340*, 8–14.

(86) Chong, J. H.; MacLachlan, M. J. *Inorg. Chem.* **2006**, *45*, 1442–1444.
(87) Wen, M.; Munakata, M.; Li, Y. Z.; Suenaga, Y.; Kuroda-Sowa, T.; Maekawa, M.; Anahata, M. *Polyhedron* **2007**, *26*, 2455–2460.
(88) Hoffmeister, E.; Kropp, J. E.; McDowell, T. L.; Michel, R. H.; Rippie, W. L. *J. Polym. Sci., Part A: Polym. Chem.* **1969**, *7*, 55-&.
(89) Kasashima, Y.; Kaneda, T.; Saito, G.; Akutsu, F.; Naruchi, K.; Miura, M. *Macromol. Chem. Phys.* **1994**, *195*, 2693–2697.
(90) Akutsu, F.; Saito, G.; Miyamoto, M.; Kasashima, Y.; Inoki, M.; Naruchi, K. *Macromol. Chem. Phys.* **1996**, *197*, 2239–2245.
(91) Akutsu, F.; Inoki, M.; Kondo, M.; Inagawa, T.; Kayaki, K.; Kasashima, Y. *Polym. J.* **1997**, *29*, 1023–1028.
(92) Zhang, Q. Y.; Li, S. H.; Li, W. M.; Zhang, S. B. *Polymer* **2007**, *48*, 6246–6253.
(93) Long, T. M.; Swager, T. M. *Adv. Mater.* **2001**, *13*, 601–604.
(94) Hilton, C. L.; Jamison, C. R.; Zane, H. K.; King, B. T. *J. Org. Chem.* **2009**, *74*, 405–407.
(95) Long, T. M.; Swager, T. M. *J. Am. Chem. Soc.* **2003**, *125*, 14113–14119.
(96) Rifai, S.; Breen, C. A.; Solis, D. J.; Swager, T. M. *Chem. Mater.* **2006**, *18*, 21–25.
(97) Tsui, N. T.; Torun, L.; Pate, B. D.; Paraskos, A. J.; Swager, T. M.; Thomas, E. L. *Adv. Funct. Mater.* **2007**, *17*, 1595–1602.
(98) Swager, T. M. *Acc. Chem. Res.* **2008**, *41*, 1181–1189.
(99) Tsui, N. T.; Yang, Y.; Mulliken, A. D.; Torun, L.; Boyce, M. C.; Swager, T. M.; Thomas, E. L. *Polymer* **2008**, *49*, 4703–4712.
(100) Hart, H.; Shamouilian, S.; Takehira, Y. *J. Org. Chem.* **1981**, *46*, 4427–4432.
(101) Hart, H.; Bashirhashemi, A.; Luo, J.; Meador, M. A. *Tetrahedron* **1986**, *42*, 1641–1654.
(102) Hart, H. *Pure Appl. Chem.* **1993**, *65*, 27–34.
(103) Chong, J. H.; MacLachlan, M. J. *Chem. Soc. Rev.* **2009**, *38*, 3301–3315.
(104) Williams, V. E.; Swager, T. M. *Macromolecules* **2000**, *33*, 4069–4073.
(105) Yang, J. S.; Yan, J. L. *Chem. Commun.* **2008**, 1501–1512.
(106) Lee, D. W.; Swager, T. M. *Synlett* **2004**, 149–154.
(107) Nesterov, E. E.; Zhu, Z. G.; Swager, T. M. *J. Am. Chem. Soc.* **2005**, *127*, 10083–10088.
(108) Zhao, D.; Swager, T. M. *Macromolecules* **2005**, *38*, 9377–9384.
(109) Zhao, D. H.; Swager, T. M. *Org. Lett.* **2005**, *7*, 4357–4360.
(110) Chen, Z. H.; Bouffard, J.; Kooi, S. E.; Swager, T. M. *Macromolecules* **2008**, *41*, 6672–6676.
(111) Venugopalan, P.; Burgi, H. B.; Frank, N. L.; Baldridge, K. K.; Siegel, J. S. *Tetrahedron Lett.* **1995**, *36*, 2419–2422.
(112) Perepichka, D. F.; Bendikov, M.; Meng, H.; Wudl, F. *J. Am. Chem. Soc.* **2003**, *125*, 10190–10191.
(113) Thomas, S. W.; Long, T. M.; Pate, B. D.; Kline, S. R.; Thomas, E. L.; Swager, T. M. *J. Am. Chem. Soc.* **2005**, *127*, 17976–17977.
(114) Chong, J. H.; Ardakani, S. J.; Smith, K. J.; MacLachlan, M. J. *Chem.—Eur. J.* **2009**, *15*, 11824–11828.
(115) Ghanem, B. S.; Msayib, K. J.; McKeown, N. B.; Harris, K. D. M.; Pan, Z.; Budd, P. M.; Butler, A.; Selbie, J.; Book, D.; Walton, A. *Chem. Commun.* **2007**, 67–69.
(116) Barton, T. J.; Bull, L. M.; Klemperer, W. G.; Loy, D. A.; McEnaney, B.; Misono, M.; Monson, P. A.; Pez, G.; Scherer, G. W.; Vartuli, J. C.; Yaghi, O. M. *Chem. Mater.* **1999**, *11*, 2633–2656.
(117) Opella, S. J.; Frey, M. H. *J. Am. Chem. Soc.* **1979**, *101*, 5854–5860.
(118) Horvath, G.; Kawazoe, K. *J. Chem. Eng. Jpn.* **1983**, *16*, 470–475.
(119) Friedman, L.; Logullo, F. M. *J. Am. Chem. Soc.* **1963**, *85*, 1549-&.
(120) Ostaszewski, R. *Tetrahedron* **1998**, *54*, 6897–6902.
(121) Goossens, R.; Smet, M.; Dehaen, W. *Tetrahedron Lett.* **2002**, *43*, 6605–6608.
(122) Shklyaev, Y. V.; Nifontov, Y. V. *Russ. Chem. Bull.* **2002**, *51*, 844–849.
(123) Aalten, H. L.; Vankoten, G.; Grove, D. M.; Kuilman, T.; Piekstra, O. G.; Hulshof, L. A.; Sheldon, R. A. *Tetrahedron* **1989**, *45*, 5565–5578.
(124) Aliev, A. E.; Harris, K. D. M.; Champkin, P. H. *J. Phys. Chem. B* **2005**, *109*, 23342–23348.
(125) Oki, M.; Matsusue, M.; Akinaga, T.; Matsumoto, Y.; Toyota, S. *Bull. Chem. Soc. Jpn.* **1994**, *67*, 2831–2837.
(126) Oki, M.; Nishino, M.; Kaieda, K.; Nakashima, T.; Toyota, S. *Bull. Chem. Soc. Jpn.* **2001**, *74*, 357–361.
(127) Suzuki, F.; Oki, M.; Nakanishi, H. *Bull. Chem. Soc. Jpn.* **1974**, *47*, 3114–3120.
(128) Yamamoto, G.; Oki, M. *Bull. Chem. Soc. Jpn.* **1983**, *56*, 2082–2085.
(129) Burgess, C. G. V.; Everett, D. H. *J. Colloid Interface Sci.* **1970**, 33.
(130) Texier-Mandoki, N.; Dentzer, J.; Piquero, T.; Saadallah, S.; David, P.; Vix-Guterl, C. *Carbon* **2004**, *42*, 2744–2747.
(131) Wong-Foy, A. G.; Matzger, A. J.; Yaghi, O. M. *J. Am. Chem. Soc.* **2006**, *128*, 3494–3495.
(132) Lin, X.; Jia, J. H.; Zhao, X. B.; Thomas, K. M.; Blake, A. J.; Walker, G. S.; Champness, N. R.; Hubberstey, P.; Schroder, M. *Angew. Chem., Int. Ed.* **2006**, *45*, 7358–7364.
(133) Ben, T.; Ren, H.; Ma, S. Q.; Cao, D. P.; Lan, J. H.; Jing, X. F.; Wang, W. C.; Xu, J.; Deng, F.; Simmons, J. M.; Qiu, S. L.; Zhu, G. S. *Angew. Chem., Int. Ed.* **2009**, *48*, 9457–9460.
(134) Wood, C. D.; Tan, B.; Trewin, A.; Su, F.; Rosseinsky, M. J.; Bradshaw, D.; Sun, Y.; Zhou, L.; Cooper, A. I. *Adv. Mater.* **2008**, *20*, 1916–1921.
(135) Nijkamp, M. G.; Raaymakers, J.; van Dillen, A. J.; de Jong, K. P. *Appl. Phys. A-Mater. Sci. Process* **2001**, *72*, 619–623.
(136) Rivera-Ramos, M. E.; Ruiz-Mercado, G. J.; Hernandez-Maldonado, A. J. *Ind. Eng. Chem. Res.* **2008**, *47*, 5602–5610.
(137) McKeown, N. B.; Ghanem, B.; Msayib, K. J.; Budd, P. M.; Tattershall, C. E.; Mahmood, K.; Tan, S.; Book, D.; Langmi, H. W.; Walton, A. *Angew. Chem., Int. Ed.* **2006**, *45*, 1804–1807.
(138) Makhseed, S.; Samuel, J. *Chem. Commun.* **2008**, 4342–4344.
(139) Germain, J.; Hradil, J.; Frechet, J. M. J.; Svec, F. *Chem. Mater.* **2006**, *18*, 4430–4435.
(140) Germain, J.; Svec, F.; Fréchet, J. M. J. *PSME Prepr.* **2007**, 97.
(141) Lee, J. Y.; Wood, C. D.; Bradshaw, D.; Rosseinsky, M. J.; Cooper, A. I. *Chem. Commun.* **2006**, 2670–2672.
(142) Yang, Z. X.; Xia, Y. D.; Mokaya, R. *J. Am. Chem. Soc.* **2007**, *129*, 1673–1679.
(143) Chen, B. L.; Ockwig, N. W.; Millward, A. R.; Contreras, D. S.; Yaghi, O. M. *Angew. Chem., Int. Ed.* **2005**, *44*, 4745–4749.
(144) Latroche, M.; Surble, S.; Serre, C.; Mellot-Draznieks, C.; Llewellyn, P. L.; Lee, J. H.; Chang, J. S.; Jhung, S. H.; Ferey, G. *Angew. Chem., Int. Ed.* **2006**, *45*, 8227–8231.